10.48047/jocaaa.2017.23.07.01

Microwave-Assisted Synthesis and Characterization of $BaAl_2Ti_6O_{16}$ Hollandite for Cesium Immobilization in High-Level Nuclear Waste

B. M. Patil

Department of Chemistry, The Institute of Science, Mumbai-400032, Maharashtra, India

Corresponding author e-*mail address*: *bmpatilisc77@gmail.com*

Abstract

In this study, $BaAl_2Ti_6O_{16}$ hollandite, a principal phase of Synroc ceramics, was synthesized via a microwave-assisted tartrate precursor method. This approach offers advantages such as rapid volumetric heating, reduced processing time, enhanced phase purity, and fine particle size distribution. The as-prepared precursor underwent thermal decomposition between 300–600 °C, with TG–DTA analysis revealing complete organic removal at 600 °C. X-ray diffraction (XRD) confirmed the formation of single-phase nanocrystalline $BaAl_2Ti_6O_{16}$ at 600 °C. FT-IR spectroscopy corroborated the decomposition of the tartrate precursor and the establishment of the hollandite framework. Morphological analysis using FE-SEM and TEM demonstrated nearly spherical nanoparticles in the 20–160 nm size range, with high uniformity and polycrystalline structure. Cylindrical pellets fabricated from the synthesized powder were sintered at 1250 °C for 5 h, resulting in dense compacts with >98% of theoretical density. Thermodilatometry revealed a linear thermal expansion coefficient of $7.47 \times 10^{-6}\,K^{-1}$, indicating excellent thermal stability suitable for high-temperature applications. The combination of high density, structural integrity, and controlled microstructure confirms the potential of microwave-synthesized $BaAl_2Ti_6O_{16}$ as a robust material for cesium immobilization in HLW, contributing to safer and more sustainable nuclear waste management strategies. This study demonstrates the effectiveness of the microwave-assisted tartrate precursor route in producing high-quality hollandite ceramics with promising structural and functional properties for advanced nuclear applications

Key words

Hollandite, Microwave-Assisted Synthesis, Nuclear Waste, Immobilization, Nanocrystalline Ceramics

Introduction

10.48047/jocaaa.2017.23.07.01

The rapid growth of industrialization, urbanization, and population has resulted in a global surge in energy demand. Conventional fossil fuels, such as coal, oil, and natural gas, continue to dominate the energy landscape; however, their extensive use has led to serious environmental issues including greenhouse gas emissions, global warming, and depletion of natural resources [1, 2]. To address the escalating global energy crisis, there is a continuous search for sustainable, efficient, and clean energy alternatives. Among the available energy sources—solar, wind, hydro, geothermal, and nuclear—nuclear energy stands out due to its high energy density and low greenhouse gas emissions during operation [3-5]. Despite these advantages, nuclear energy presents significant challenges, primarily related to the generation and safe management of radioactive waste. High-level nuclear waste (HLW), which includes long-lived radionuclides such as cesium-137 (Cs-137) and strontium-90 (Sr-90), poses a serious environmental and radiological hazard if not properly immobilized [6,7]. The immobilization of HLW into stable and durable solid matrices is, therefore, a critical step in nuclear waste management [7]. Various materials, including borosilicate glasses and crystalline ceramics, have been explored for this purpose. However, glasses often suffer from poor chemical durability and low thermal stability when exposed to high radiation doses [8]. Consequently, crystalline ceramic waste forms, such as Synroc (synthetic rock), have emerged as promising alternatives due to their high chemical durability, thermal stability, and structural flexibility [9]. Synroc, originally developed by Ringwood and co-workers in the late 1970s [10], is a multiphase titanate-based ceramic designed to immobilize a wide range of radioactive elements by incorporating them into specific crystalline phases. Typical Synroc formulations consist of four main phases: perovskite ($CaTiO_3$), zirconolite ($CaZrTi_2O_7$), and hollandite ($BaAl_2Ti_6O_{16}$) and TiO_2. Among these, the hollandite phase plays a crucial role due to its tunnel-type crystal structure, which can accommodate large monovalent cations such as Cs^+ within its lattice channels, making it highly effective for cesium immobilization [11,12].

Several synthesis routes have been employed for the preparation of hollandite-type $BaAl_2Ti_6O_{16}$, including solid-state reaction, sol–gel, coprecipitation, hydrothermal, and combustion methods [13–16]. However, these conventional approaches often require high calcination temperatures, long processing times, and result in poor homogeneity or grain coarsening. In recent years, microwave-assisted synthesis has gained attention as an advanced method due to its advantages such as rapid volumetric heating, reduced reaction time, fine particle size, and improved phase purity [17]. Moreover, the use of tartrate precursor routes enhances compositional uniformity

10.48047/jocaaa.2017.23.07.01

and lowers synthesis temperature, making the process more energy-efficient and environmentally friendly.

In the present study, $BaAl_2Ti_6O_{16}$ hollandite has been synthesized via a microwave-assisted tartrate precursor method. The prepared samples were characterized using TG-DTA (for thermal behavior), XRD (for phase identification), FESEM and TEM (for morphological and microstructural analysis), density measurements and thermal expansion to evaluate the thermal compatibility and structural stability of the synthesized material. The developed $BaAl_2Ti_6O_{16}$ ceramic is proposed as a potential candidate for immobilization of cesium from high-level nuclear waste, contributing to safer and more sustainable nuclear waste management strategies.

2. Materials and Methods

2.1 Synthesis of $BaAl_2Ti_6O_{16}$

All reagents used were of analytical reagent (AR) grade and utilized without further purification. Titanium (III) chloride solution (15% $TiCl_3$, S.D. Fine Chemicals Ltd., Mumbai, India), aluminum nitrate nonahydrate ($Al(NO_3)_3 \cdot 9H_2O$), barium nitrate ($Ba(NO_3)_2$), and tartaric acid (Merck, India) were used as starting materials. In a typical synthesis, equimolar aqueous solutions of $Ba(NO_3)_2$ and $Al(NO_3)_3 \cdot 9H_2O$ were added dropwise to the $TiCl_3$ solution under continuous magnetic stirring. The reaction was distinctly exothermic, leading to the oxidation of Ti^{3+} to Ti^{4+}, thereby maintaining the overall stoichiometric ratio of Ba:Al:Ti = 1:2:6. The progressive color change of the solution from violet (indicative of Ti^{3+}) to greenish-yellow confirmed the complete oxidation of titanium ions. Subsequently, an aqueous solution of tartaric acid was introduced into the reaction mixture while maintaining a molar ratio of Ba:Al:Ti:Tartaric acid = 1:2:6:9. The solution was stirred continuously to ensure homogeneous mixing and complexation among the metal ions and organic ligand. The resulting uniform sol was then dried in an air oven at 200 °C to obtain a free-flowing brown precursor powder. The dried precursor was subjected to microwave-assisted thermal treatment in the temperature range of 300–600 °C. Complete thermal decomposition of the tartrate precursor occurred at 600 °C within 1 h, yielding a single-phase nanocrystalline $BaAl_2Ti_6O_{16}$ powder. The schematic representation of the synthesis route is depicted in Figure 1. The resultant BAT powder was finely

10.48047/jocaaa.2017.23.07.01

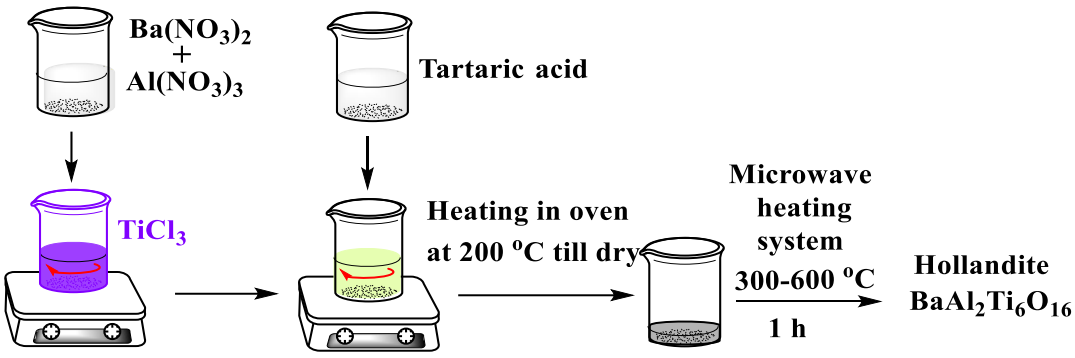

Figure 1: Schematic of the synthesis of $BaAl_2Ti_6O_{16}$ in Microwave heating.

ground in an agate mortar to ensure uniform particle size distribution. The powder was then compacted into cylindrical pellets (8 mm diameter and 5 mm thickness) using a uniaxial hydraulic press under an applied pressure of 50 MPa. The green pellets were subsequently sintered in air at 1250 °C for 5 h, with a controlled heating rate of 10 °C min^{-1}. The sintering process promoted densification and enhanced the phase purity and crystallinity of the hollandite-structured $BaAl_2Ti_6O_{16}$.

2.2 Characterization

The thermal behavior of the as-prepared tartrate precursor was examined by simultaneous thermogravimetric–differential thermal analysis (TG–DTA) using a DIAMOND TG–DTA instrument (PerkinElmer, Germany) under flowing air atmosphere. The analysis provided detailed insights into the decomposition pattern, mass loss events, and phase formation mechanisms occurring during thermal treatment of the precursor. The phase evolution and crystalline structure of the $BaAl_2Ti_6O_{16}$ powders calcined at various temperatures were analyzed by X-ray diffraction (XRD) using a Rigaku Miniflex II diffractometer equipped with a monochromatic Cu Kα radiation source (λ = 0.15405 nm). The obtained diffraction patterns were compared with standard JCPDS data to identify the crystalline phases and confirm the formation of the hollandite structure. The microstructural and morphological characteristics of the $BaAl_2Ti_6O_{16}$ powders at different calcination stages were studied using field emission scanning electron microscopy (FE-SEM, JEOL JSM-7600F). To obtain detailed information on crystallite size, lattice fringes, and particle morphology, high-resolution transmission electron microscopy (HR-TEM) was performed using a FEI Tecnai G2 F30 microscope operating at an accelerating voltage of 300 kV.

10.48047/jocaaa.2017.23.07.01

The linear thermal expansion behavior of the sintered BAT pellets was measured using a push-rod thermodilatometer (NETZSCH DIL 402 Classic) in the temperature range of 30 °C to 950 °C, with a controlled heating rate of 10 °C min^{-1} in air. This study provided insights into the thermal stability and structural integrity of the hollandite phase under elevated temperatures. The bulk density of the sintered $BaAl_2Ti_6O_{16}$ ceramics was determined using the Archimedes liquid displacement method, employing deionized water as the immersion medium. The measured density values were used to evaluate the degree of sintering and densification of the ceramic pellets

3. Results and Discussion

3.1: Thermal Analysis

The simultaneously recorded thermogravimetric (TG) and differential thermal analysis (DTA) curves of the barium aluminum titanyl tartrate (BATT) precursor are presented in Fig. 2. The TG curve shows a three-step mass loss behavior. The first step, up to 150 °C, corresponds to the removal of physically adsorbed and lattice water, accounting for approximately 8 wt% weight loss. This dehydration process is followed by two partially overlapping decomposition steps associated with the thermal degradation of the organic tartrate groups. No further weight change was observed beyond 500 °C, indicating complete decomposition of the tartrate precursor and formation of intermediate oxide species. The DTA curve exhibits a broad exothermic region extending from 25 to 1100 °C, with two superimposed exothermic peaks centered around 200 °C and 350 °C, respectively. These peaks are attributed to the oxidation of gaseous products such as CO and H_2 evolved during the decomposition process. The broad exothermic background suggests a gradual crystallization of the intermediate and final oxide phases formed upon heating.

X-ray diffraction (XRD) analysis of the product obtained at 500 °C confirmed its amorphous nature. The persistence of a broad exothermic signal beyond this temperature range indicates the crystallization of the amorphous/glassy phase, which is consistent with the XRD results (Fig. 3). Upon calcination at 800 °C, well-crystallized nanosized $BaAl_2Ti_6O_{16}$ phase was obtained, confirming the completion of crystallization and phase formation.

10.48047/jocaaa.2017.23.07.01

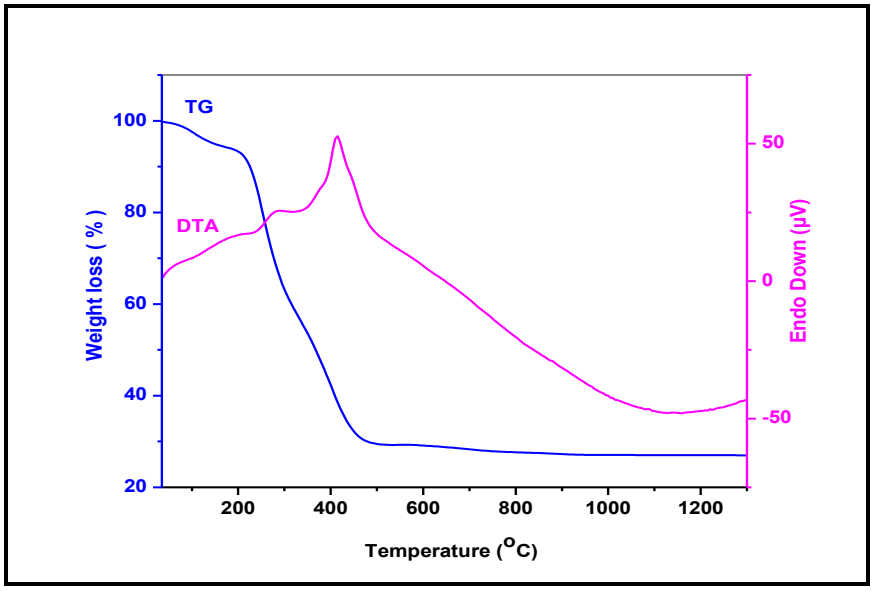

Fig. 2: Simultaneous TG- DTA curve of Barium Aluminum Titanyl tartrate precursor (BATT) precursor

3.2 X-ray Diffraction Analysis:

The X-ray diffraction (XRD) patterns of the products obtained by calcination of the barium aluminum titanyl tartrate (BATT) precursor at various temperatures using a microwave heating technique are shown in Fig. 3. As observed from the diffraction profiles, the material obtained after thermal treatment up to 500 °C remains essentially amorphous, indicating that the decomposition of the organic matrix and oxide phase formation are not yet complete at this stage. A gradual evolution of diffraction peaks was noted with increasing temperature, suggesting the onset of crystallization beyond 600 °C. At 600 °C, the XRD pattern (Fig. 3e) exhibits sharp and well-defined reflections corresponding to the Hollandite-type structure of $BaAl_2Ti_6O_{16}$, which is in good agreement with the standard JCPDS card No. 33-0133 [15]. The absence of any secondary peaks confirms the formation of a single-phase nanocrystalline product. The crystallite size, estimated from the line broadening of the most intense diffraction peaks using the Scherrer equation, indicates the formation of fine nanosized crystallites. It is noteworthy that the crystallization of $BaAl_2Ti_6O_{16}$ occurred at a significantly lower temperature (≈600 °C) under microwave-assisted calcination compared to the conventional thermal method, where the formation of the same phase typically requires higher temperatures. This enhancement can be attributed to the rapid volumetric heating and enhanced diffusion kinetics promoted by the microwave irradiation, leading to accelerated phase formation and improved homogeneity of the product.

10.48047/jocaaa.2017.23.07.01

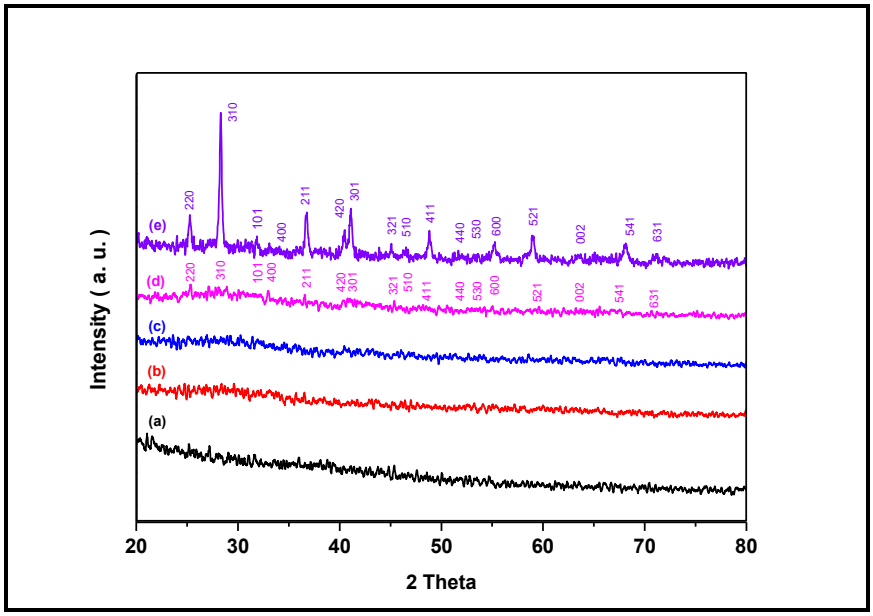

Fig. 3: XRD patterns of BATT precursor (a) as prepared (b) 300°C (c) 400°C (d) 500°C e) 600°C for 1hour

3.3 FT-IR spectral analysis

The Fourier Transform Infrared (FTIR) spectra of the as-prepared and annealed Barium aluminium titanyl tartrate (BATT) precursor samples, heated at various temperatures (300–600 °C) in a microwave system, are shown in Figure 4. In the as-prepared precursor, a broad absorption band at 3514 cm^{-1} corresponds to the O–H stretching vibrations of adsorbed water and hydroxyl groups. The band at 1730 cm^{-1} arises from the C=O stretching vibration of the tartrate moiety, while the absorption at 1627 cm^{-1} is due to H–O–H bending and overlapping C=O stretching vibrations. The bands at 1449, 1361, 1126, and 1077 cm^{-1} confirm the presence of oxalate and tartrate groups, whereas absorptions at 910, 830, 731, 647, 539, and 449 cm^{-1} are attributed to mixed O–C=O and M–O vibrations, indicating the chelation of Ti^{4+}, Al^{3+}, and Ba^{2+} ions with the organic ligands. On annealing at 300 °C, the O–H stretching band shifts to 3423 cm^{-1}, signifying partial dehydration, while the C–O and C=O related vibrations near 1400 and 1623 cm^{-1} persist, suggesting incomplete decomposition of the organic moieties. At 400 °C, the reduction in the intensity of organic bands (1385–1530 cm^{-1}) and the disappearance of the C=O band at 1730 cm^{-1} indicate progressive oxidation and decomposition of the tartrate and oxalate groups. A new band at 531 cm^{-1} corresponds to M–O stretching vibrations, marking the initiation of oxide phase formation. At 500 °C, most organic bands vanish, while new peaks at 541 and 610 cm^{-1} are observed, associated with Ti–O–Ti lattice vibrations, signifying the

10.48047/jocaaa.2017.23.07.01

crystallization of the inorganic framework. Weak bands in the 800–875 cm^{-1} region suggest the transient presence of carbonate intermediates. At 600 °C, all organic-related absorptions disappear, and strong bands at 511 and 610 cm^{-1} are characteristic of Ti–O lattice vibrations, accompanied by a residual O–H stretching band at 3456 cm^{-1}. These observations confirm the complete decomposition of the organic precursor and the formation of nanocrystalline $BaAl_2Ti_6O_{16}$.

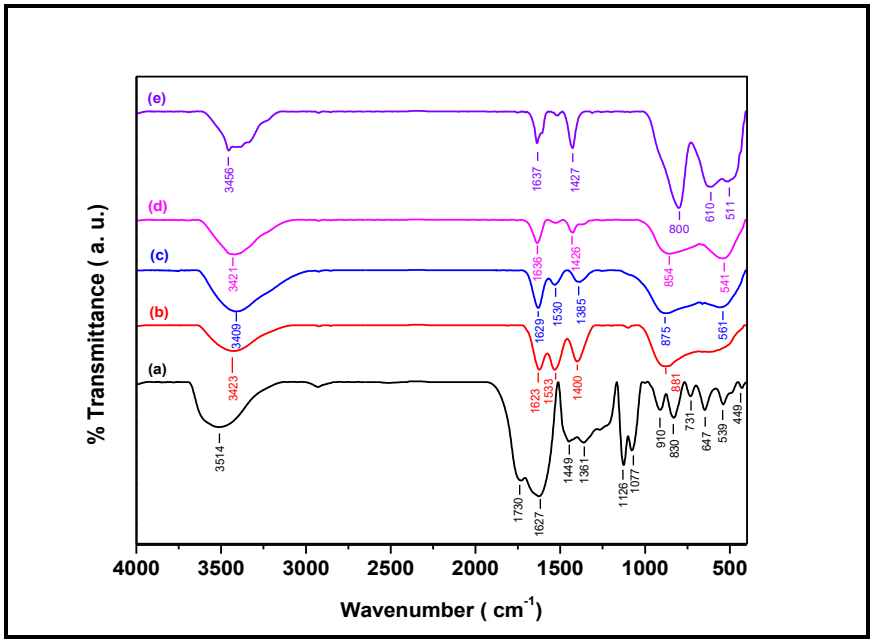

Fig. 4: IR spectra of BATT precursor calcined in Microwave heating at (a) as prepared (b) 300ºC (c) 400ºC (d) 500ºC and (e) 600ºC for one hour.

3.4 Particle size distribution Analysis:

The particle size distribution of $BaAl_2Ti_6O_{16}$ powders synthesized by microwave-assisted heating of the precursor at 600 °C for one hour is presented in Figure 5. The distribution curve exhibits a relatively narrow particle size range, indicating uniformity in the particle growth under microwave processing conditions. The majority of the particles are distributed between 120 and 160 nm, with a distinct peak centered around 149 nm, representing the average particle size of the synthesized $BaAl_2Ti_6O_{16}$ nanoparticles. The observed particle size is in close agreement with the results obtained from FE-SEM micrographs (Figure 5b), which show the formation of nearly spherical, well-crystallized nanoparticles in the same size range. The narrow size distribution further suggests that microwave heating promotes homogeneous nucleation and controlled particle growth, minimizing agglomeration and leading to uniform

10.48047/jocaaa.2017.23.07.01

nanocrystalline morphology. This consistency between dynamic light scattering (DLS) analysis and SEM observations confirms the reliability of the synthesis process and highlights the effectiveness of microwave-assisted heating in producing fine, uniformly sized $BaAl_2Ti_6O_{16}$ nanocrystals.

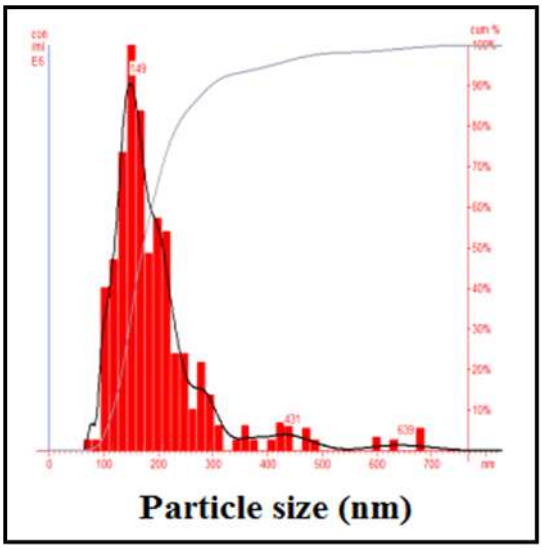

Fig. 5: Particle Size distribution

3.5 Field Emission-Scanning Electron Microscopy (FE-SEM) Analysis:

The surface morphology and microstructural evolution of $BaAl_2Ti_6O_{16}$powders, synthesized by microwave-assisted calcination of the Barium aluminium titanyl tartrate (BATT) precursor at different temperatures, were examined using Field Emission Scanning Electron Microscopy (FE-SEM), as shown in Figure 6. At 500 °C, the micrograph (Figure 6a) reveals a glassy and amorphous morphology, indicating that the precursor has undergone partial decomposition but has not yet developed a well-defined crystalline structure. The surface appears smooth and continuous, characteristic of an amorphous intermediate phase.

When the calcination temperature is increased to 600 °C, the morphology changes markedly (Figure 6b). The microstructure shows the formation of well-defined, nanocrystalline particles with nearly spherical morphology. The particle size is found to range between 20 and 160 nm, indicating significant nucleation and growth of crystallites. This observation is consistent with the average particle size distribution obtained from the nanoparticle size analyzer (Figure 6b), confirming the nanoscale nature of the $BaAl_2Ti_6O_{16}$ powder synthesized under microwave conditions.

10.48047/jocaaa.2017.23.07.01

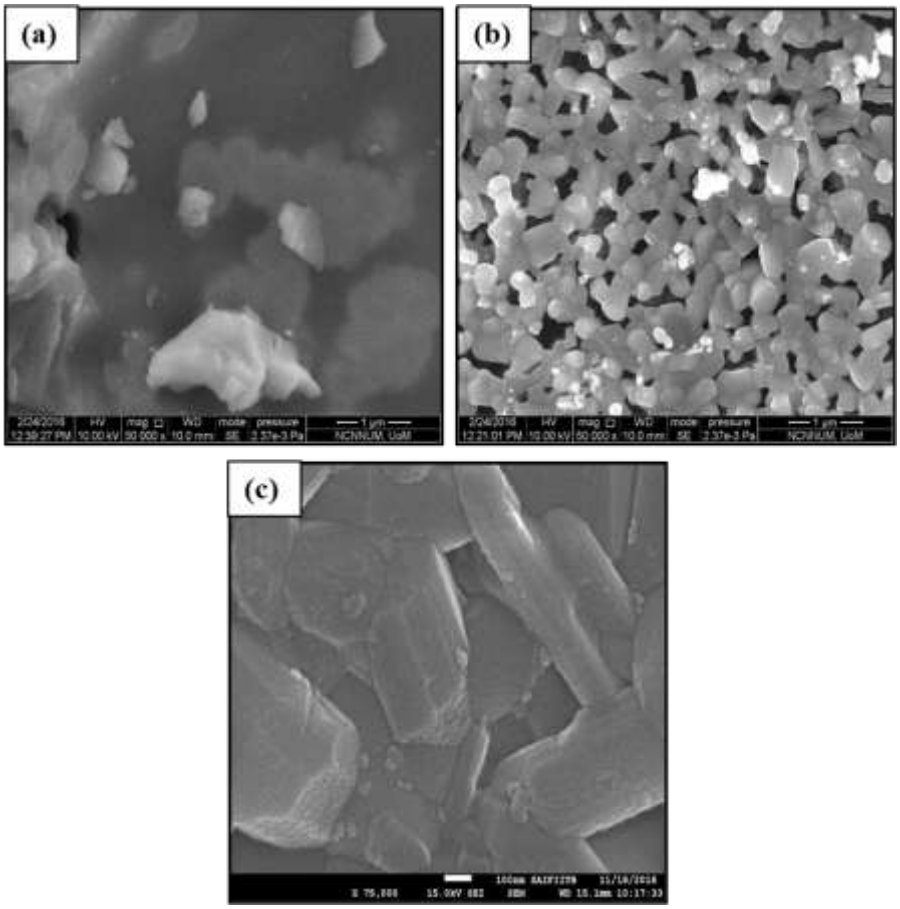

Fig. 6: SEM images of $BaAl_2Ti_6O_{16}$ at (a) 500ºC (b) 600ºC for one hour and (c) sintered pellet at 1250 ºC

Further, the densification behavior of the $BaAl_2Ti_6O_{16}$ powder, calcined at 600 °C and sintered at 1250 °C, is depicted in Figure 6c. The micrograph reveals that the nanocrystalline particles undergo agglomeration and coalescence during sintering, leading to the formation of a dense microstructure with reduced porosity. This densification process enhances the interparticle bonding and promotes the development of a compact ceramic body, characteristic of the well-sintered $BaAl_2Ti_6O_{16}$ phase. Overall, the FE-SEM analysis clearly illustrates the structural evolution of $BaAl_2Ti_6O_{16}$ from an amorphous phase to a nanocrystalline structure and finally to a dense sintered body, depending on the annealing and sintering condition.

3.6 Transmission Electron Microscopy (TEM) and selected Area electron diffraction (SAED) analysis:

The TEM micrograph and SAED pattern of $BaAl_2Ti_6O_{16}$ synthesized by heating the BATT precursor at 600 °C in a microwave oven for one hour, followed by sonication in deionized water for five minutes, are shown in Figure 7. The TEM image (Figure 7a) reveals a

10.48047/jocaaa.2017.23.07.01

heterogeneous morphology consisting of a few larger particles along with a dominant population of nanoparticles below 50 nm in size. The corresponding SAED pattern (Figure 7b) displays diffused concentric diffraction rings, confirming the polycrystalline nature of the $BaAl_2Ti_6O_{16}$ nanoparticles and indicating the presence of a large number of small crystallites. Overall, the SAED ring pattern confirms that the $BaAl_2Ti_6O_{16}$ nanoparticles obtained via microwave synthesis retain a polycrystalline structure, consistent with the formation of nanocrystalline oxide phases.

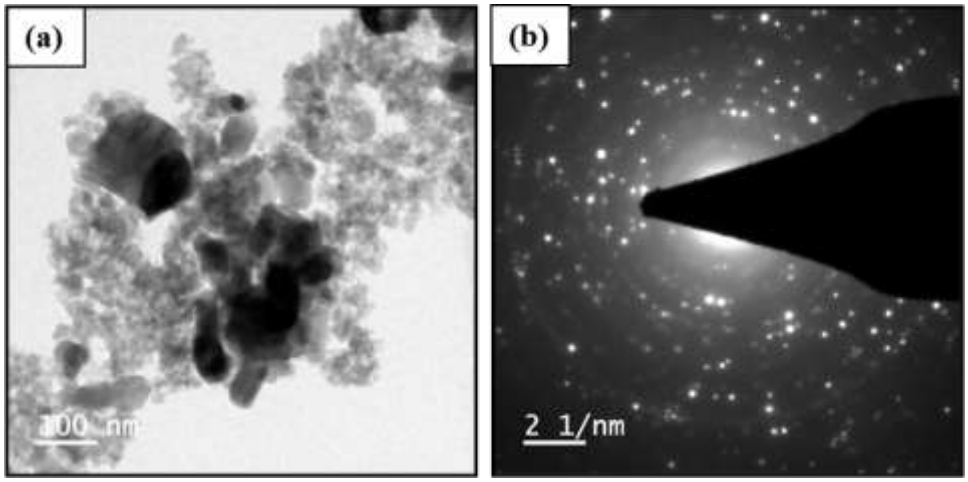

Fig. 7: (a) TEM and (b) SAED images of $BaAl_2Ti_6O_{16}$

3.7 Shrinkage and Thermal Expansion:

The shrinkage behavior of cold-pressed $BaAl_2Ti_6O_{16}$ pellets was analyzed using thermodilatometry to determine the optimum sintering temperature for achieving maximum densification. Cylindrical pellets were prepared from $BaAl_2Ti_6O_{16}$ powder obtained via microwave synthesis, with 5 wt.% polyvinyl alcohol (PVA) added as a temporary binder. The mixture was uniaxially compacted under a pressure of 4 tons/in² to form uniform green pellets.

The shrinkage curve of the $BaAl_2Ti_6O_{16}$ pellet is presented in Figure 8. The results indicate that the green body begins to exhibit noticeable shrinkage at approximately 900 °C, marking the onset of significant densification. A steady increase in shrinkage is observed beyond this temperature, attributed to enhanced diffusion and neck growth among the nanoparticles. Based on the thermodilatometric data, the optimum sintering temperature was determined to be 1250 °C, which provides adequate thermal energy for rapid densification and effective grain boundary diffusion within a reasonable holding time. At this temperature, the

10.48047/jocaaa.2017.23.07.01

$BaAl_2Ti_6O_{16}$ nanoparticles consolidate efficiently into a dense ceramic structure, suitable for subsequent microstructural and electrical property investigations.

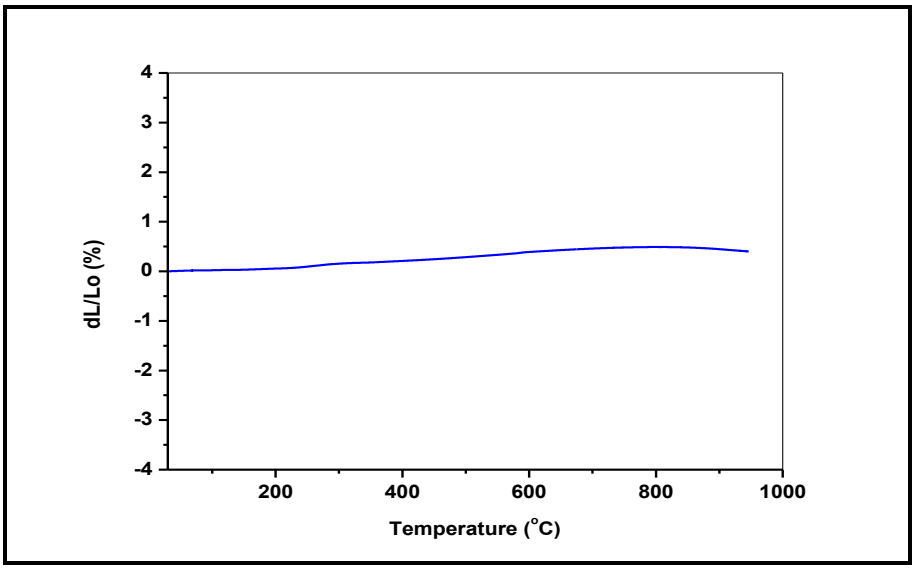

Fig. 8: Shrinkage pattern of hollandite green pellet of BAT at 600ºC in Microwave oven for one hour.

The bulk thermal expansion behavior of hollandite pellets, prepared via thermal decomposition of the precursor and subsequently sintered in a microwave oven at 1250 °C for 5 h in air, is presented in Fig. 9. The dilatometric measurements were carried out to determine the linear thermal expansion characteristics of the sintered pellets. From the recorded dilatometric curves, the average linear thermal expansion coefficient (α) of the microwave-sintered hollandite pellets was calculated to be 7.47×10^{-6} K^{-1}. This value is consistent with the previously reported values in the literature [18, 19], indicating that the microwave-assisted sintering process does not adversely affect the intrinsic thermal expansion properties of hollandite. The observed thermal expansion behavior confirms the structural stability of the material over the temperature range studied, which is crucial for potential high-temperature applications.

The dilatometric curve (Fig. 9) shows a nearly linear expansion with temperature, suggesting homogeneous densification during sintering and the absence of significant microstructural defects such as cracks or pores that could contribute to anomalous expansion behavior. These results demonstrate that microwave sintering can effectively produce hollandite ceramics with thermal expansion characteristics comparable to those prepared by conventional methods.

10.48047/jocaaa.2017.23.07.01

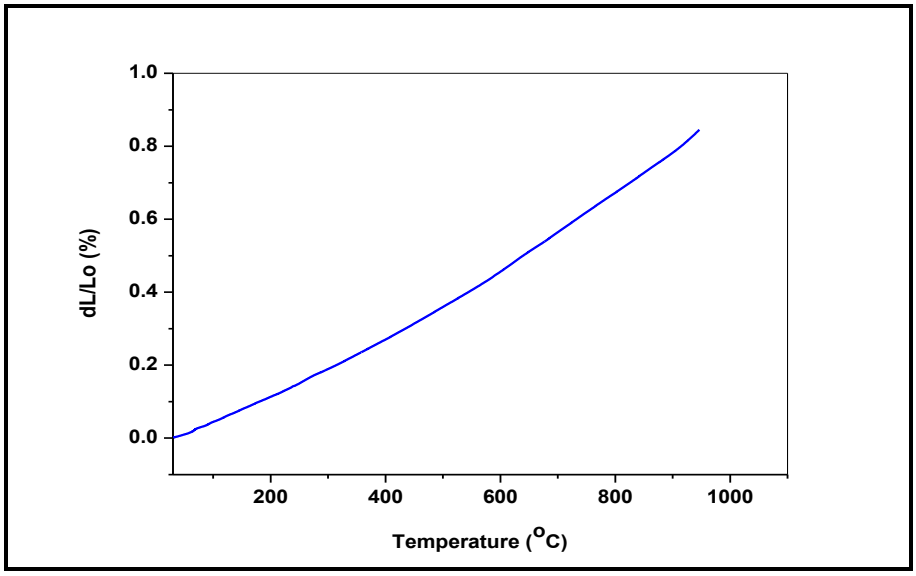

Figure 9: The thermal expansion of the sintered pellets

3.8 Density of Analysis:

The density of the sintered hollandite pellets was determined using the liquid displacement method. The measured density values of the pellets are in good agreement with previously reported values [18,19], confirming the reliability of the preparation and sintering procedures. The results clearly indicate that hollandite powder synthesized from the tartrate precursor via microwave heating exhibits excellent sinterability, producing sintered compacts with densities exceeding 98% of the theoretical value when sintered at 1250 °C for 5 h. This high level of densification demonstrates the suitability of the tartrate-derived hollandite powder for the fabrication of dense ceramic components with minimal porosity. These findings underscore the effectiveness of the chosen precursor and microwave-assisted sintering protocol in producing high-density hollandite ceramics, which is essential for achieving desirable physical and functional properties in potential applications, particularly in next-generation nuclear technology

3.9 Conclusion

$BaAl_2Ti_6O_{16}$ hollandite was successfully synthesized via a microwave-assisted tartrate precursor method, offering a rapid, energy-efficient, and environmentally friendly route for nanocrystalline ceramic production. Thermal analysis (TG–DTA) confirmed complete decomposition of the organic precursor by 600 °C, while XRD verified the formation of single-phase nanocrystalline hollandite. Morphological studies using FE-SEM and TEM revealed

10.48047/jocaaa.2017.23.07.01

uniform, nearly spherical nanoparticles ranging from 20–160 nm, demonstrating controlled particle growth and high homogeneity achieved through microwave processing. Sintered pellets exhibited densities exceeding 98% of the theoretical value, indicating excellent sinterability and minimal porosity. Thermodilatometric measurements showed a linear thermal expansion coefficient of $7.47 \times 10^{-6}\,K^{-1}$, confirming the structural stability of the sintered hollandite across a broad temperature range, crucial for thermal compatibility in nuclear waste immobilization. The combination of high densification, nanoscale microstructure, and thermal stability underscores the potential of $BaAl_2Ti_6O_{16}$ hollandite as a robust matrix for Cesium immobilization in high-level nuclear waste**.** Overall, this work demonstrates that the microwave-assisted tartrate precursor route provides a reliable and efficient approach to produce high-quality hollandite ceramics with controlled morphology, phase purity, and functional properties, supporting safer, sustainable, and next-generation nuclear waste management strategies.

Acknowledgments

The author would like to acknowledge Dr. Pravin Walke, Centre of nanoscience and Nanotechnology for SEM images, SAIF, IIT, Mumbai for TG-DTA, FTIR spectra, Dilatometry study and TEM images and Dr. S. R. Dharwadkar for valuable guidance

References:

[1] J. Diefenderfer, Vipin Arora and L. E. Singer, “International Energy Outlook 2016.

[2] Panwar, N. L., Kaushik, S. C., & Kothari, S.. "Role of renewable energy sources in environmental protection: A review." Renewable and Sustainable Energy Reviews, 15(3), (2011) 1513.

[3] R. Saidur, M.R. I, N.A. Rahim, K.H. Solangi, A review on global wind energy policy, Renewable and Sustainable Energy Reviews, 14 (7), (2010) 1744.

[4] Manfred Lenzen, Life cycle energy and greenhouse gas emissions of nuclear energy: A review, Energy Conversion and Management, 49 (8) (2008) 2178.

[5] Abhilash Kantamneni, Richelle Winkler, Lucia Gauchia, Joshua M. Pearce, merging economic viability of grid defection in a northern climate using solar hybrid systems, Energy Policy, 95 (2016) 378.

[6] Ewing, R. C. “Long-term storage of spent nuclear fuel.” Nature Materials, 14(3), (2015)

10.48047/jocaaa.2017.23.07.01

252.

[7] Christophe Poinssot, Stéphane Gin, Long-term Behavior Science: The cornerstone approach for reliably assessing the long-term performance of nuclear waste, Journal of Nuclear Materials, 420, (1–3), (2012) 182.

[8] Michael I. Ojovan, William E. Lee, An Introduction to Nuclear Waste Immobilisation 2nd Edition, Elsevier (2013)

[9] A. E. Ringwood, S. E. Kesson, N. G. Ware, W. Hibberson, and A. Major, Immobilization of high-level nuclear waste in SYNROC, Nature, 278 (5701) (1979) 219.

[10] A. E. Ringwood, S. E. Kessom, N. G. Ware, W. O. Hibberson, and A. Major, The SYNROC process: A geochemical approach to nuclear waste immobilization, A. Geochemical Journal, 13 (1979) 141.

[11] A. E. Ringwood, V. M. Oversby, S. E. Kesson, W. Sinclair, N. Ware, W. Hibberson, A. Major, Nucl. Chem. Waste Manag., 2 (4) (1981) 287.

[12] A.Y. Leinkugel-le-Cocq, P. Deniard, S. Jobie, R. Cerny, F. Bart, and H. Emerich, Synthesis and characterization of hollandite-type material intended for the specific containment of radioactive cesium, J. Solid State Chem, 179 (10) (2006) 3196.

[13] I. W. Donald, B. L. Medtacalfe and K. N. J. Taylor, The immobilization of high level radioactive wastes using ceramics and glasses, J. Mater. Sci., 32 (22) (1997) 5851.

[14] R. W. Cheary, An X-ray structural analysis of cesium substitution in the barium hollandite phase of synroc, J. Nucl. Mater., 125 (1984) (2007) 236.

[15] H. Xu, G. C. C. Costa, C. R. Stanek and A. Navrotsky, Structural Behavior of Ba1.24Al2.48Ti5.52O16 Hollandite at High Temperature: An In Situ Neutron Diffraction Study, J. Am. Cream. Sco., 98 (2015) 255.

[16] M. Muthuraman, N. A. Dhas, and K. C. Patil, Combustion synthesis of oxide materials for nuclear waste immobilization, Bull. Mater. Sci., 17 (6) (1994) 977.

[17] B. M. Patil, R. S. Srinivasa, S. R. Dharwadkar, Synthesis of CaTiO3 from calcium titanyl oxalate hexahydrate (CTO) as precursor employing microwave heating technique, Bull. Mater. Sci., 30 (3), (2007), 225.

[18] M. Muthuraman, K.C. Patil, S. Senbagaraman, and A.M. Umarji, Sintering,

10.48047/jocaaa.2017.23.07.01

microstructural and dilatometric studies of combustion synthesized synroc phases, Mater. Res. Bull, 31 (11) (1996) 1375.

[19] C. L. Hoenig, H. W. Newkirk, R. A. Otto, R. L. Brady, A. E. Brown, A. R. Ulrich, R. C. Lum, Mechanical and Thermophysical Properties of Hot-Pressed SYNROC B, Lawrence Livermore Laboratory, University of California, Livermorc, California, 1-15 (1981).